CODEN:LUTEDX/(TEIE-5287)/1-064/(2011)

Industrial Electrical Engineering and Automation

Rotary Position Sensors

Comparative study of different rotary position sensors for electrical machines used in an hybrid electric vehicle application

Christer Ebbesson

Division of Industrial Electrical Engineering and Automation
Faculty of Engineering, Lund University

Rotary Position Sensors
Comparative study of different rotary position sensors for electrical machines used in an hybrid electric vehicle application

Christer Ebbesson
Faculty of Engineering,
Lund University,
Lund,
Sweden,
christer.ebbesson@gmail.com

August 29, 2011

Abstract

Today, many projects about Electric Vehicles (EVs) and Hybrid Electric Vehicles (HEVs) are in progress within the automotive industry. Fuel-efficiency and reduction of carbon dioxide emissions from vehicles are the main targets. This thesis is within in one of these projects that is called electric All Wheel Drive (eAWD) at BorgWarner TorqTransfer Systems AB.

A key parameter to perform an accurate and efficient control of an electric machine is the position sensor. The sensor measures the angular position of the rotor shaft and there are several ways and techniques to do this.

This thesis aims to compare different common position sensors and identify "new" sensor techniques by performing a literature study, model and simulate sensors and test an electric machine with different sensors implemented. Various enhancement methods to improve the position information and prediction are also evaluated.

The electric motor prototype used in the eAWD project has different position sensors implemented and these are simulated in Matlab/Simulink together with the system model of the electric machine and control system. Tests are also performed and compared to the simulation results.

The results show on best performance when using the resolver as position sensor. The Hall-effect sensor can be improved with an observer, but the observer is not suitable for this specific type of Torque Vectoring (TV) application. The Hall-effect sensor has a speed dependent torque ripple that leads to harmonics at frequencies that relates to the speed of the unit which may causes problems, such as mechanical resonances in the system. There are several "new" sensor techniques based on the theory of eddy-currents that may be of interest since they are said to be more optimized for EV and HEV applications.

Preface

This master thesis has been carried out at BorgWarner TorqTransfer Systems AB in Landskrona, Sweden. It has been made possible by excellent supervision of the Department of Industrial Electrical Engineering and Automation (IEA) at the Faculty of Engineering at Lund University (LTH).

It has been a great and challenging to work with industrial development and to apply what I have learnt during my engineering studies.

Finally, I would like to thank:

Jonas Ottosson (BorgWarner) and Francisco Márquez (IEA), for providing great and helpful supervision.

Gustaf Lagunoff (BorgWarner), for his supervision and support during the construction of the test setup and during the test phase.

My family and friends for their support.

Christer Ebbesson
Lund, August 2011

Contents

List of Figures

List of Tables

List of Acronyms

ADC Analog-to-Digital Conversion

eAWD electric All Wheel Drive

EMC Electromagnetic Compatibility

EMI Electromagnetic Interference

EMPOS Electric Motor Position Sensor

EV Electric Vehicle

FFT Fast Fourier Transform

HEV Hybrid Electric Vehicle

ICE Internal Combustion Engine

IGBT Insulated-Gate Bipolar Transistor

ISG Integrated Starter-Generator

LED Light Emitting Diode

PCB Printed Circuit Board

PLL Phase-Locked Loop

PMSM Permanent Magnet Synchronous Machine

PWM Pulse-Width Modulation

RDC Resolver-to-Digital Conversion

SSI Synchronous Serial Interface

TV Torque Vectoring

VR Variable Reluctance

Chapter 1

Introduction

One of today's biggest concerns are the climate and the global warming. Many claim that by our combustion of fossil fuels and thereby increasing carbon dioxide emissions have caused, or will cause, a large global climate change.

The field of automotive development is one of many areas where research projects about fuel-efficiency and other various projects about reduce carbon dioxide emissions from vehicles are in progress.

This chapter presents one of this projects within the automotive industry and how it relates to the topic of this thesis.

1.1 Background

BorgWarner Inc. is a world leading company in powertrain solutions, i.e. engine, transmission, drive shafts, differentials, four-wheel-drive systems etc. At BorgWarner TorqTransfer Systems AB (former Haldex Traction Systems AB) facilities in Landskrona, Sweden, development of a prototype called eAWD is in progress. The eAWD project is an electric drive system to be used in EV and HEV applications. Shortly, the current system consist of two Permanent Magnet Synchronous Machines (PMSMs), one PMSM at 85 kW that is used for propulsion and one PMSM at 10 kW that is used for TV[1]. Another electrical machine that also is a part of the concept is the Integrated Starter-Generator (ISG) that is connected to the Internal Combustion Engine (ICE) and which can both charge the battery and supply power to the two electrical motors. The system car integration layout is shown in figure 1.1. A position sensor is needed for each machine in order to control it accurately and with high dynamics.

[1]Torque vectoring is a new technology that provides the option to vary the amount of power sent to each wheel.

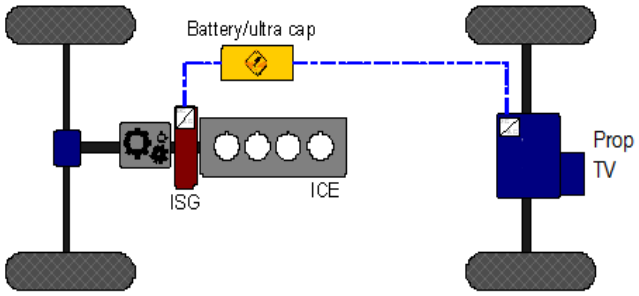

Figure 1.1: Car block description.

This thesis will only focus on the PMSM for the TV application. This application is a bit special since it changes the direction of rotation fast during operation which the position sensor needs to be able to manage.

There are high demands on the sensors, since they have a large impact on the control and performance of the PMSMs. However, on the other hand, this application is within the automotive industry and every part needs to be as cost-effective as possible.

1.2 Objectives

This work aims to compare and evaluate different rotary position sensors that can be used to control a PMSM. The work consists of a theoretical part with literature study of different sensors and a more practical part with implementation and testing. Sensors are modelled and simulated in MathWorks® Matlab®/Simulink®. Several tests are performed on a PMSM with different sensors implemented and compared with the sensor simulations. Different hardware and software enhancement techniques are also included. The results and conclusions are going to be presented in terms of accuracy, dynamic limitations, resolution, robustness, torque quality and price. The effect on the torque quality, for each sensor, is also studied. Furthermore, other sensor techniques that may suit the eAWD project will also be investigated.

1.3 Outline

This is a short outline and overview of the chapters of this report.

- Chapter 2 covers the fundamental theory of different rotary position sensors and enhancement techniques. The sensors that are used for the eAWD project, together with various other sensors, are explained.
- Chapter 3 consists of sensor models, system model, system simulations, test cases, test system setup and system testing approaches.
- Chapter 4 presents the simulation and testing results.
- Chapter 5 considers the conclusions and future work within this and related topics.

Chapter 2

Theoretical Background

A rotary position sensor is a unit that can measure the angular position of something that rotates, e.g. an electric motor shaft of a PMSM. Since the control of a PMSM is done by controlling the current in its three phases, it is necessarily to always know the right position to be able to know which of the phases to control in each time instance. This is explained more in detail in the coming sections.

Rotary position sensors can be divided into different groups depending on how they physical sense the position. The physical methods can be; mechanical, optical, inductive/magnetic or capacitive. Each of these main groups can be divided in two subgroups; absolute and incremental. If the sensor is absolute, it can give the real position at any given time and then it is called to be "true absolute position at power-on". This can be compared with the incremental sensor that only can be used to increase or decrease a counter containing the position information. Even if a non-volatile memory[1] is used to store the position information when there is no power connected to the system, the incremental sensor will not register changes in the position during that time. Another way to compare the different sensors are in the way they can be mounted and how the reading of the position is done. Mounting designs can be either through-shaft, partial-through-shaft or end-of-shaft and the actual rotor shaft position reading can be done either axially, i.e. in line with the rotor shaft or radially, i.e. orthogonally to the rotor shaft.

One of the PMSM prototypes used in the eAWD project at BorgWarner is equipped with three different position sensors and therefore it is those that this thesis will mostly be focused on. Although, other types of sensors that could be suitable for the eAWD prototypes will be taken into consideration, as well as various enhancement techniques to improve the estimation of the position. The theory of this and more are explained in this chapter.

[1] A non-volatile memory is a computer memory that can retain stored information without any power supply.

2.1 The Resolver/Synchro

The simplest way to describe the resolver is to compare it with a small electric motor or a rotating transformer. It consist of two stator windings and one rotor (excitation) winding. By applying an excitation signal on the rotor winding, this signal will by induction, occur in the stator windings. Depending on the position of the rotor winding, related to the stator windings, the angle of the output signal will change. Let

$$U_{ref} = E\sin(\omega_{exc}t) \tag{2.1}$$

be the excitation signal with a frequency of ω_{exc}. The signal that the two secondary signal in the stator are sensing can be expressed as

$$U_{sin} = KE\sin(\omega_{exc}t)\sin(\theta) \tag{2.2}$$

$$U_{cos} = KE\sin(\omega_{exc}t)\cos(\theta) \tag{2.3}$$

where K is the transformer ratio, E is the amplitude of the excitation signal and θ is the actual rotor position [8, p. 2-3]. The equations 2.2 and 2.3 are visualised in figure 2.1 together with modulated signals containing the information about the angle θ.

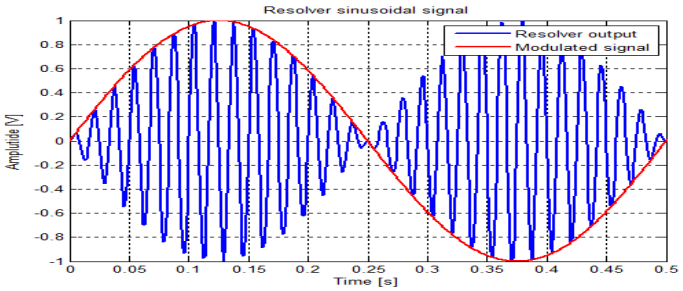

(a) Sine.

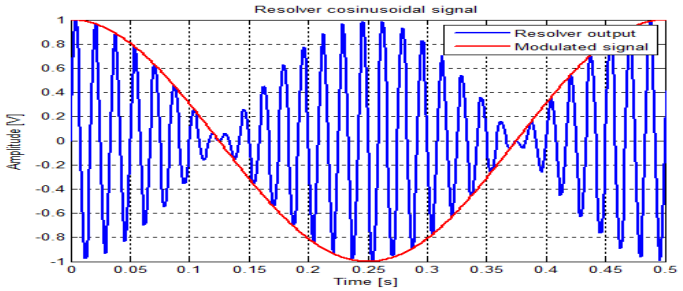

(b) Cosine.

Figure 2.1: Resolver output signals.

The resolver needs a Resolver-to-Digital Conversion (RDC) in order to demodulate the resolver output signals and to generate the excitation signals. The RDC is described in section 2.1.3.

2.1.1 The Variable Reluctance (VR) Resolver

A variant of the resolver is the VR resolver. The excitation windings are placed in the stator instead of in the rotor and a sinusoidal shape disc is placed in the rotor. Due to Maxwell's equations, a magnetic flux always forms a closed loop where the reluctance[2] is lowest. So when the disc rotates, and the air gap between the disc and the stator output windings varies and thus varies the path where the reluctance is lowest. This makes the output signals varies in a sinusoidal way.

A principle layout of the resolver and the VR resolver shown in figure 2.2.

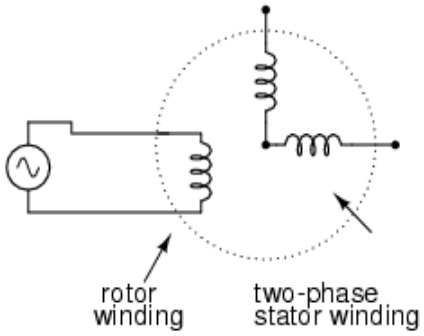

(a) Resolver

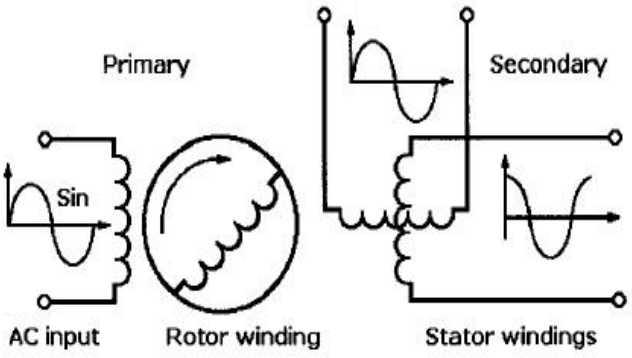

(b) VR resolver

Figure 2.2: Resolver vs. VR resolver [16], [6].

[2]Magnetic reluctance is analog with the electric resistance

A VR resolver can be design in several way. Two examples with 1 pole pair and 4 pole pairs are shown in appendix A.1.

2.1.2 The Synchro

Another more complex and advanced type of resolver is the synchro. It has the same basic construction and functionality as a regular resolver, but it has three stator windings instead of two. The three windings are placed with 120° apart and thus it has three signal outputs. The synchro provides a signal with higher resolution and is often used in the aerospace industry. A layout of the synchro is shown in figure 2.3 [16].

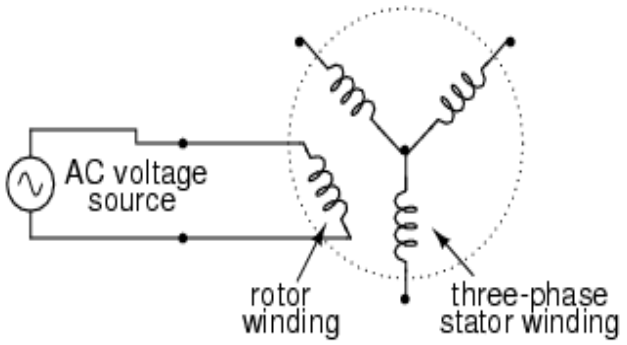

Figure 2.3: Synchro schematic [16].

2.1.3 Resolver-to-Digital Conversion (RDC)

As described in section 2.1, the output signals from a resolver are amplitude modulated signals. This signals needs to be demodulated and converted to digital signals before those can be used for control. There are several method proposals when converting the resolver signals to digital data. The conversion can be done by either undersampling or oversampling [15, p. 5].

When using undersampling the sine and cosine signals must both be sampled with the same frequency as the excitation signal frequency. To avoid generating two separate signals (one signal for excitation and one for sampling), a square wave signal can be generated and used for sampling. The reference signal for excitation can be generated by filtering the square wave signal with a first order low-pass filter. This signal will be a sinusoidal signal with the same frequency as the square wave but with a phase delay (and lower amplitude that may be taken into consideration). The filtering shall be done so the output signal has the maximal value at the falling flank of the square wave. If the RDC is sampling

on this falling flank, the absolute maximal values of the modulated signal will be sampled [7]. The square wave and the low-pass filtered signals are shown in figure 2.4.

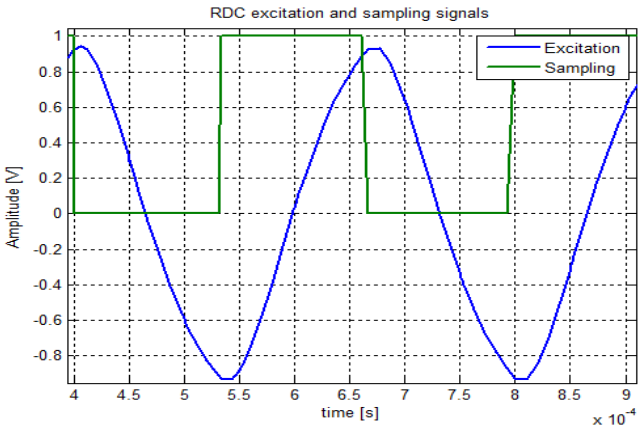

Figure 2.4: Resolver model excitation and sampling signals.

2.2 The Hall-effect sensor

The Hall-effect was discovered in year 1879 by Edwin Hall and explains what is happening when a magnetic field is applied orthogonally to a metal plate. If a constant current flows through a piece of metal, as shown in figure 2.5, the perpendicular voltage over the same metal will change with the variation in strength of the applied magnetic field. Equation 2.4 shows how the Hall-voltage varies [12, p. 1-2].

$$U_H = \frac{IB}{q_0 N d} \tag{2.4}$$

where I is the current [A], B is the applied magnet field [T], q_0 is the charge of a electron ($1.60 \cdot 10^{-19}$ [C]), N is the carrier density [carriers/cm^3] and d is the thickness of the conductor [m].

This effect can be used to sense variations in magnetic fields, e.g. from a rotating magnet. One way to use this sensor in a PMSM is to mount three sensors together with filtering and amplification on one electrical turn of the machine and let those sense the magnetic field of the permanent magnets. In the theoretical case the sensor signals will look like those in figure 2.6a and if these are decoded to a position it will give the behaviour like in figure 2.6b.

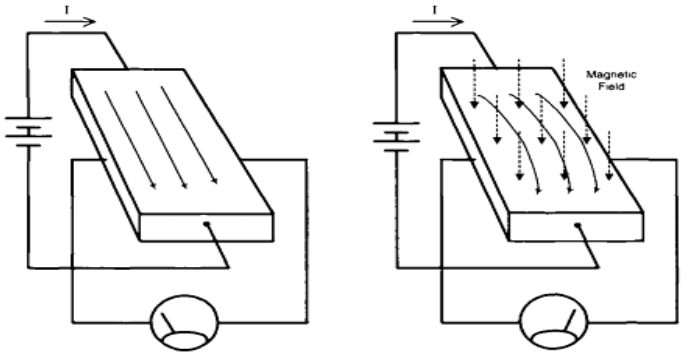

Figure 2.5: The Hall-effect [12, p. 1].

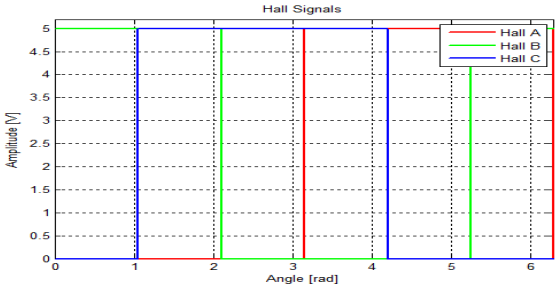

(a) Hall signals.

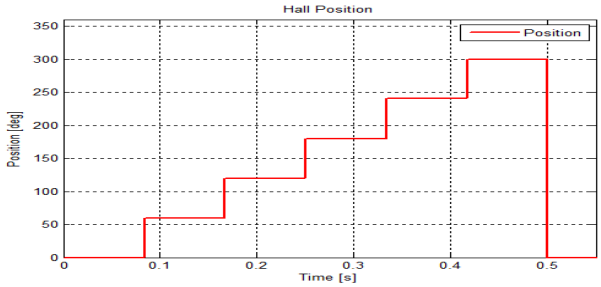

(b) Position of PMSM.

Figure 2.6: One electric rotation of a PMSM with three Hall-effect sensors.

A Hall-effect sensor can be made very cheap and small. Basically, this sensor is analog, but can be used to operate digitally by a Schmitt trigger output. Figure 2.7 shows a common discrete Hall-effect sensor. Hall-effect sensors have also the advantages of being insensitive to e.g., dust, humidity, vibration and have a constant over time behaviour.

Its primary disadvantage is the limitation in measuring distance. It does not

work well with distances over 10 cm (depending on the magnet field). Another limitation is related to the Hall voltages U_H (equation 2.4) where both the carrier density N and the resistance (and thus the current I) of the material are depending on the temperature [12].

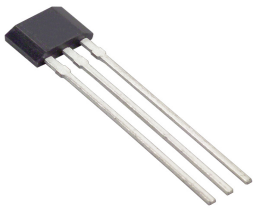

Figure 2.7: A Hall-effect sensor.

2.3 The Encoder

The basic function of the Encoder is that a certain binary encoded pattern or track on the rotor can be sensed and decoded to a position. The physical sensing method can either be mechanical, optical or inductive/magnetic.

- A mechanical method can be used by letting brushes sense a conductive track placed on the rotor. A drawback with this method is that the brushes are noisy and wear out and that a rough environment have a negative impact on the performance.
- Different optical methods can also be used. One way is to send light with a Light Emitting Diode (LED) to a reflective track placed on the rotor and sense the reflections. Another optical way is to send light through the target track and sense the light coming out on the other side with a photo-diode. The drawbacks with this method is that dirt can interfere with the light and that the LED can break.
- It is also possible to use a magnetic method. The target track pattern can be either magnetic or magnetic absorbing material that is sensed by a Hall-effect sensor. A drawback with this method is that other external magnetic sources can create interference with the sensor.

The Encoder can be either absolute or incremental. The sensing target pattern can be mounted axial or radial, i.e. the reading or sensing of the rotor can be in line with or orthogonally to the rotating shaft. Figure 2.8 shows two target pattern that could be used for those three sensing methods explained above. The pattern consist of four Gray-encoded[3] bits and can be used to relate to the position. Gray coding is preferred since changes in two or more

[3]Gray code is binary numeral system where only one bit is changed between two adjacent values.

bits during one state passage could give several combinations depending in which order the bits changes.

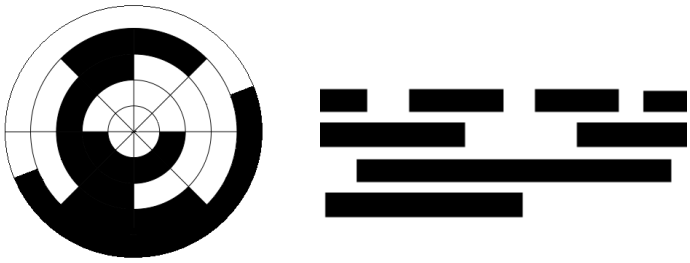

(a) Disc layout. (b) Track layout.

Figure 2.8: 4-bit Gray-encoded pattern.

The resolution is depending on how many bits (tracks) that is used. It can be calculated by using equation 2.5 where N is the number of bits [2].

$$Resolution = \frac{360^\circ}{2^{\mathrm{N}}}[\mathrm{deg}] \tag{2.5}$$

Depending on which sensing technique that is used, the encoder comes with different advantages and disadvantages. The magnetic or optical method are to prefer since those are more robust. A disadvantage can be seen in equation 2.5. To reach high resolution the number of bits needs to be high (10-12 bits) and the sensor may be large or the tracks have to be small.

2.4 Other sensors

There are some other sensors that are very interesting and may suit the eAWD application. This report will only consider the general functionality of these sensors and does not addresses simulation and testing.

2.4.1 The SKF bearing sensor

SKF has recently developed a bearing unit with an integrated position sensor which is shown in figure 2.9. It consist of a set (usually 3-7) of analog Hall-effect sensor units which together with amplification and output signal filtering provides a pure analog position output. The numbers and placements of the Hall-effect sensor units are depending on the physical size of the bearing and the number of poles used in the application. The output can be either single-ended or differential sinusoidal signals and the limitation in resolution is only depending on the Analog-to-Digital Conversion (ADC) in the control application, but the resolution will also be affected by the physical size, the number of poles and the number of Hall-effect sensors [10].

(a) Cross section. (b) Complete unit.

Figure 2.9: The SKF bearing sensor [10].

The PMSM is in any case in need of bearings, so this solution comes with the advantage to combine a bearing with a position sensor and thus saves space and money. It also has high immunity to Electromagnetic Interference (EMI) and is not easily affected by hazard a environment due to the surrounding steel cage. It can be used in high speed operation, where the maximum speed is limited by the mechanical design rather than the electrical components [10].

2.4.2 The Sumida inductive Rotor-Position Sensor (RPS)

Sumida Components and Modules has design a inductive Rotor-Position Sensor (RPS), which they state is specially designed to work in hybrid electric vehicle applications. This sensor is based on the theory of eddy-current[4] losses. The eddy-current theory is well-known, but the application to use it to measure an angular position is a new area of use. Sumida's proposed design consist of two parts; the sensor and the target (see figure 2.10a). The sensing unit consist of an arrangement of planar coils which can contact less sense a rotating target. The target trace is shaped in a sinusoidal way and is made of a conductive material such as copper or aluminium and can be mounted in either metallic or plastic material [17, p. 5] [4].

The planar coils expose the target for a high frequency field and eddy-current is induced in the target. The eddy-current cause a opposite field which reduces the inductance in the coils. The coils are a part of a resonance circuit which changes frequency and phase as the inductance varies. This behaviour can be related to the angular position [17, p. 5].

[4]Also know as Foucault currents named after the French physicist Léon Foucault (1819 - 1868).

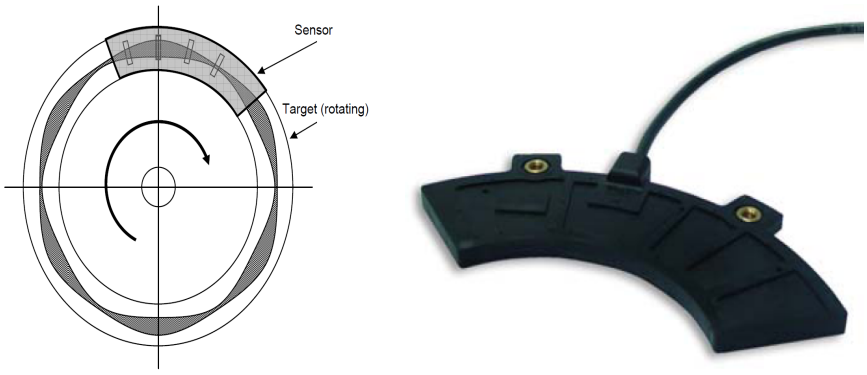

(a) Target and sensor. (b) Sensor.

Figure 2.10: Sumida Eddy current sensor [17, p. 3, 10].

Figure 2.10 shows only the axial mounted type, but it is possible to use the same technique with radial mounting which is more expensive due to more complex design but has better peformance when large axial tolerance is needed. Sumida claims that the sensor has high immunity to magnetic interference and thus it can be integrated into the motor without any shielding. That together with the segment-shaped sensor unit implies huge advantages since it saves space [17, p. 4].

2.4.3 The Electricfil Automotive EMPOS

Like Sumida, Electricfil Automotive has also developed a position sensor based on the same eddy-current principle which they call Electric Motor Position Sensor (EMPOS) (see figure 2.11). It consists of one primary and two secondary windings that are printed on a Printed Circuit Board (PCB), placed on the motor stator. On the rotor is an aluminium trace fixed. A high frequency current is feed into the primary winding that generates an alternating magnetic field which in turn causes eddy-currents. The eddy-currents generates an opposing magnetic field that can be measured as alternating voltages in the secondary windings. Integrated on the PCB are also electronics for generating the signal that are needed for excitation of the primary winding and other diagnostic functions. Electricfil Automotive implies that the EMPOS offers an accuracy of ± 1 electrical degree and is capable to handle speeds up to 20,000 RPM and is insensitive to pollution, EMI and vibrations. The sensor is thin and lightweight and the aluminium trace can easily be designed and integrated to the rotor shaft by punching. Today is the development of this sensor only in prototype stage but the mass production is scheduled for 2012 [5].

Figure 2.11: The Electricfil Automotive EMPOS [5].

2.5 Enhancement methods

Improvements can be done by using signal processing, filtering or prediction. Signal processing can be done in both hardware and software to get rid of noise, harmonics and other unwanted behaviours. It it much easier and cheaper to do this in software than in hardware.

2.5.1 The Observer

An observer is a powerful method to use for prediction of the position between two well known position states. In the Hall-effect sensor model, presented in figure 3.4, there are 30° between the states, and to estimate the position between these an observer can be used. Let

$$\theta_{obs} = \theta_{meas} + \omega_{meas} \cdot \Delta t \tag{2.6}$$

be the predicted position from the observer where θ_{meas} and $\omega_{measured}$ are the position and the speed information, respectively. In other words, the observer estimates the position between two stages based on the previous stage. This might seems like a good solution but its assumes that the speed is the same or almost the same during next state, i.e. no acceleration or retardation.

2.5.2 Filtering

In EV and HEV applications a lot of noise are present. This may have a bad effect on the position signal quality and thus filtering may be needed. Filtering can be done in several ways with different type of filters of different orders. Especially sensors without differential outputs are exposed. Filtering has to be done with caution since it will introduce signal delays and thus affects the position information in a bad way.

2.6 The PMSM

When controlling a PMSM with a position sensor as feedback, it is the electrical angle that is of interest, and not the mechanical angle. The relation between this to is $\theta_{el} = \frac{n_p}{2}\theta_{mech}$, where n_p is the number of poles.

2.6.1 Current control

The PMSM is operated by controlling a three phase current. In this setup this is done by vector control. To avoid a complex current controller a rotating coordinate system is used. In figure 2.12, there are two coordinate system. The first one is the $\alpha - \beta$ stator coordinate system which is fixed. The second is the $x - y$ rotor coordinate system which is rotating together with the rotor.

Two mathematical transforms (Clark Transform and Park Transform) are used. Let i_{sa} and i_{sb} be two of the three phase currents and assume a symmetrical three phase system. Then can the three phase system be written as a two dimensional system (equations 2.7-2.8) with the Clark Transform.

$$i_{s\alpha} = \sqrt{3/2} \cdot i_{sa} \tag{2.7}$$

$$i_{s\beta} = \frac{1}{\sqrt{2}} \cdot i_{sa} + \sqrt{2} \cdot i_{sb} \tag{2.8}$$

The Park Transform can then be used to transform the system into rotor coordinates (vectors), equation 2.9 and 2.10, where θ is angle between the two coordinate systems.

$$i_{sx} = i_{s\alpha} \cdot \cos\theta + i_{s\beta} \cdot \sin\theta \tag{2.9}$$

$$i_{sy} = i_{s\beta} \cdot \cos\theta - i_{s\alpha} \cdot \sin\theta \tag{2.10}$$

Equations 2.9-2.10 are then used as input to the current controller [7].

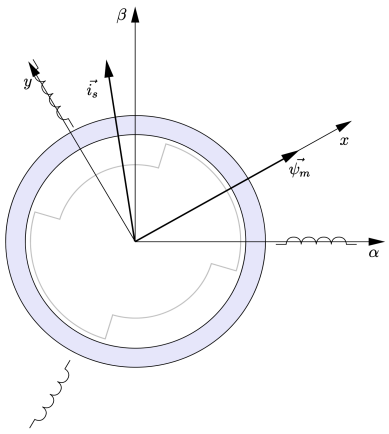

Figure 2.12: Stator and rotor coordinate systems [1, p. 254].

2.6.2 Performance

It is mainly the performance, i.e. the torque quality of the PMSM, that is of interest to measure, quantise, evaluate and compare to the associated sensor. Torque quality can be defined in many different ways. This study will address the torque quality in terms of torque ripple and torque ripple frequency contents. If steady state can be assumed, the torque ripple T_{ripple} can be defined as [13, p. 2]

$$T_{ripple} = \left| \frac{T_{max} - T_{min}}{T_{mean}} \right| \cdot 100 \, [\%] \tag{2.11}$$

Torque production

Let

$$\tau_e = \frac{3n_p}{2} \psi_R (i_q \cos\tilde{\theta} - i_d \sin\tilde{\theta}) \tag{2.12}$$

be the electrical torque of the PMSM, where n_p is the number of poles, ψ_R is the magnetic flux, i_q and i_d is the currents and $\tilde{\theta}$ is the angular position error between the two coordinate systems as explained in previous section. If the position is known with precision, the error $\tilde{\theta}$ become zero and then equation 2.12 reduces to [7, p. 228-229]

$$\tau_e = \frac{3n_p}{2} \psi_R i_q \tag{2.13}$$

Chapter 3

Methodology

This chapter presents the practical work regarding system implementation and testing such as; modeling, test cases, system specification and setup configuration.

3.1 Modeling

Based on theory and information about those sensors that are implemented in the PMSM, models of those are built in Matlab®/Simulink®. The position sensor blocks are shown in figure 3.1. The model also contains a resolver-to-digital block to demodulate and convert the resolver signal to a digital signal and a observer block connected to the Hall-effect sensor model to predict the position between the Hall states. Furthermore, blocks to support control signals and quantization are shown as well.

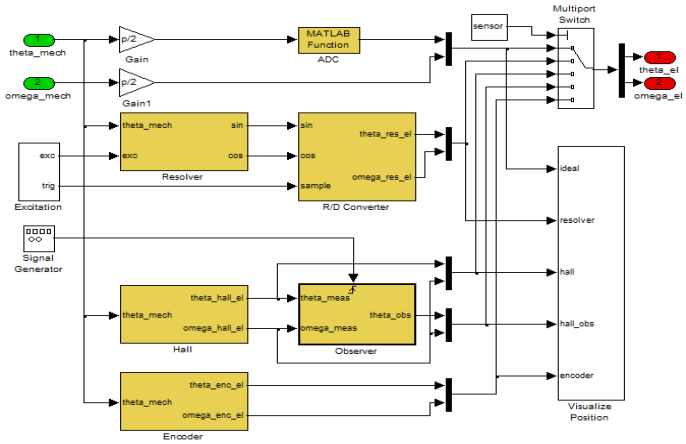

Figure 3.1: Sensor models.

These models are only based on theory and thus are ideal and without any limitations. Certain possibilities to apply errors are implemented and are explained more in detail for each sensor model.

3.1.1 The Resolver

The resolver block in figure 3.2 consist of the excitation signal as input and the modulated sinusoidal (sine and cosine) output signals.

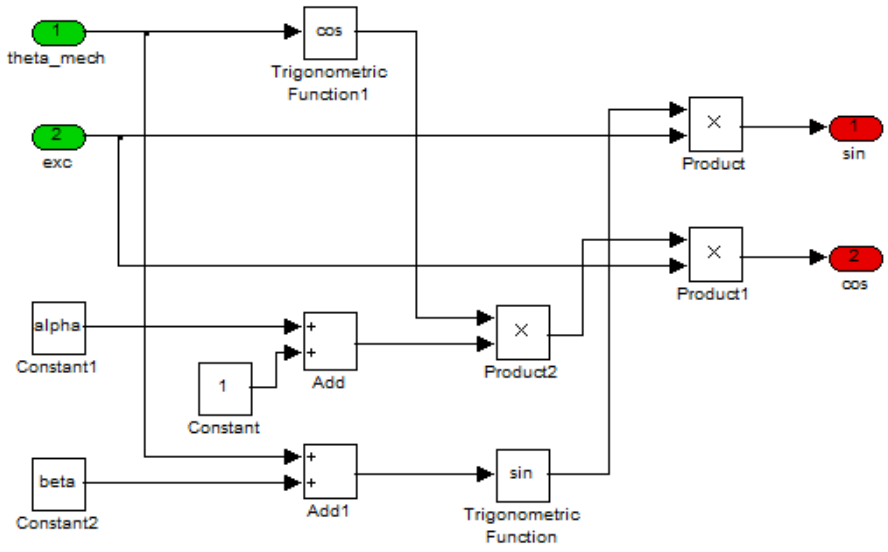

Figure 3.2: Resolver model.

It is possible to add errors such as amplitude imbalance (alpha) and imperfect quadrature (beta). Differences in amplitude of the modulated output signals results in *Amplitude imbalance* and a phase shift that is not exactly 90 degrees results in *Imperfect quadrature* [8].

Resolver-to-Digital Conversion

The RDC model is shown in figure 3.3.

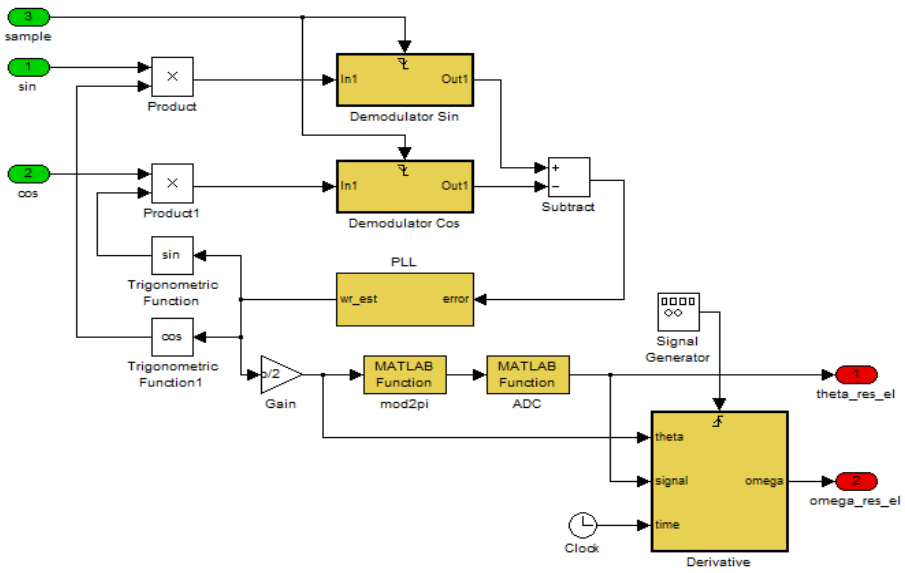

Figure 3.3: Resolver-to-Digital model.

It consists of demodulation of the sine and cosine signals, which is a simple sample-and-hold function to sample the resolver signal with the same frequency as the carrier wave (excitation) signal. The Phase-Locked Loop (PLL) is used for tracking of the resolver signal [7, p. 316-319]. Since the excitation frequency of the resolver is 5 kHz the sampling rate is the double (10 kHz) to avoid aliasing.

3.1.2 The Hall-effect sensor

The model consists of three analog Hall-effect sensor elements whose output signals are filtered. The relays acts as Schmitt triggers to make a digital output. The sensor signals are coded to states which represents an angle.

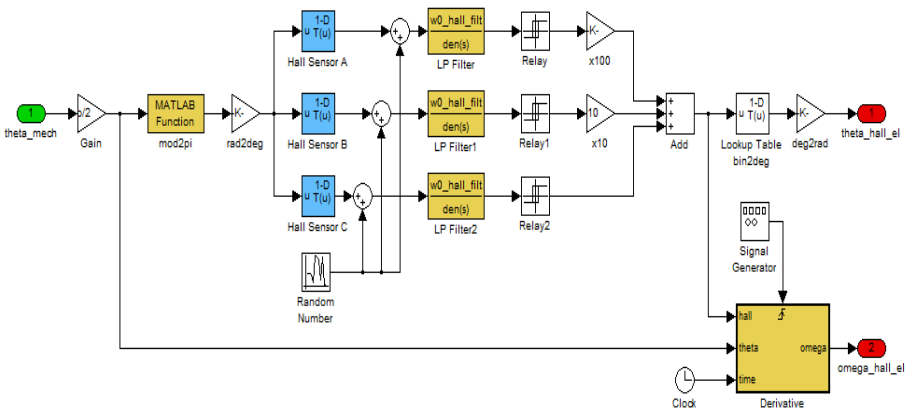

Figure 3.4: Hall-effect sensor model.

The relays triggers on positive and negative flank when the signals have the value of $e - \frac{1}{e} \approx 63.2\%$ of final value. This value is the time constant τ of the filter and can be used to simulate different time delays that occurs due to filtering.

The Observer

The observer is implemented and coded as in Program 1 below and is implemented exactly as described in section 2.5.1. It is updated with the same rate as the switching frequency (10 kHz).

Program 1 Observer model implementation.

```
function [theta_obs,timer_hall] = observer(theta_meas,omega_meas,
theta_meas_old,timer_hall_old,dtobs)

if theta_meas ~= theta_meas_old
    timer_hall = 0;
else
    timer_hall = timer_hall_old + dtobs;
end

theta_obs = theta_meas + omega_meas*timer_hall;

if theta_obs > theta_meas+pi/3
    theta_obs = theta_meas+pi/3;
elseif theta_obs < theta_meas-pi/3
    theta_obs = theta_meas-pi/3;
end
```

3.1.3 The Encoder

The encoder is modelled with a digital output where the number of bits can be changed.

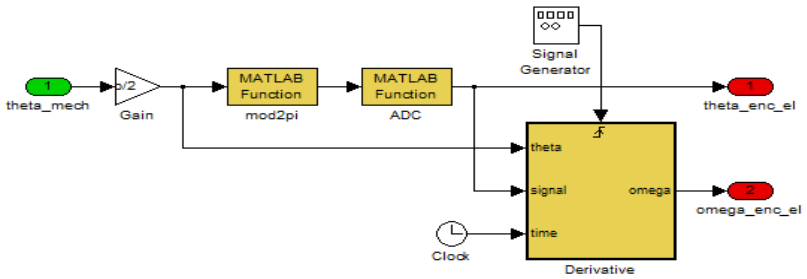

Figure 3.5: Encoder model.

3.1.4 Full system model

The position sensor block is connected to the entire system in figure 3.6. The top model consists of (from left) a current controller, a modulator, an inverter, a PMSM, position sensors and a speed controller block.

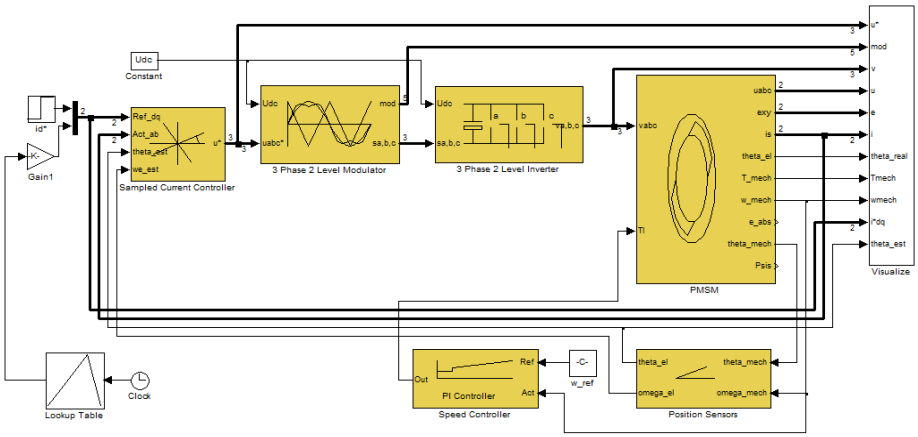

Figure 3.6: The top system model.

This model is based on the one used in the power electronics course at LTH and has been adapted to the system and PMSM unit at BorgWarner.

3.2 Implementation

3.2.1 The PMSM

The TV PMSM specification is shown in table 3.1.

Quantity	**Rating**	**Unit**
Voltage	300	V
Power	10	kW
Max speed	10,000	RPM
Number of poles	6	-
Max. peak current	38	A
Cont. current	21	A
Inertia	0.02	kgm^2
Stator resistance	0.193	Ω
Stator inductance (L_{sx}=L_{sy})	0.53	mH
Electrical torque ψ_m	0.0674	Nm/A

Table 3.1: TV motor specification.

3.2.2 Sensor implementation

The PMSM used for TV in the eAWD project has three sensors implemented; resolver, Hall-effect sensor and encoder which are explained in this section.

The Resolver

The resolver is of a variable reluctance type and is manufactured by Tamagawa Seiki CO., LTD and is custom made to suite the eAWD project. It has six poles and a maximum speed rating of 30,000 rpm. The six wires electrical interface consist of three differential signals for excitation input and sine/cosine outputs.

The Hall-effect sensor

The Hall-effect sensor unit is manufactured and supplied by Honeywell. It consist of three discrete bipolar analog Hall-effect sensors of Honeywell SS400 type. These sensors sense the permanent magnets in the PMSM rotor and are placed over one electrical period of the motor with a distance of 120 electrical degrees apart as shown in figure 3.7. These sensors can sense magnetic fields in the interval of ±70-140 G[1]. The sensors are analog, but the unit has a digital output due to build-in Schmitt triggers, and thus the unit can provide six discrete states related to the position [14].

The outputs are not filtered and operate as open-collector. This means that the output signals have to be filtered before the signal can be used. The choice of filter and filter parameters are mentioned in section 3.2.3.

[1]Gauss [G] is a unit of a magnetic field or magnetic flux density. 1 G = 10^{-4} T.

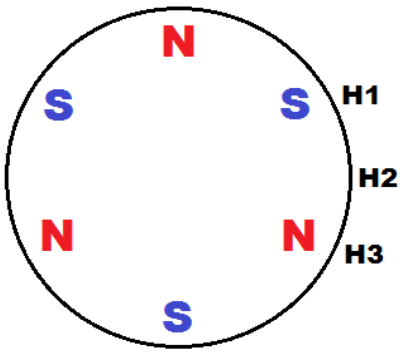

Figure 3.7: PMSM rotor and Hall-effect sensors placements.

The Encoder

A NdFeB magnet[2] of 6 mm in diameter is mounted on end of the rotor axle. To sense the rotation of this magnet and thus the rotor, the Austriamicrosystems AS5145A IC placed is next to the magnet with a distance of less than 5 mm. A layout of the placement is shown in figure 3.8. The AS5145A can measure the angular position over a full turn of 360°. According to the specification, it can provide a resolution of 0.0879°, i.e. 4096 positions per revolution [2, p. 12]. The electrical interface consist of five wires; two for power supply (+3.3V and reference ground), one input for mode selection and two for data output.

Figure 3.8: Operation of the AS5145 [2, p. 12].

This type of magnetic encoder is based on four Hall-effect sensors, but in another way than the true discrete Hall-effect sensor. The reading is done axially

[2]Neodymium magnet (2000 Gauss).

in line with the axle and thus limiting the torque transfer possibilities from that side of the axle. The analog signal from the Hall-effect sensors are amplified and processed by a DSP which can output the angular information to the Pulse-Width Modulation (PWM), Synchronous Serial Interface (SSI) and incremental output interfaces. The placement of the Hall-effect sensors in the IC is shown in figure 3.9.

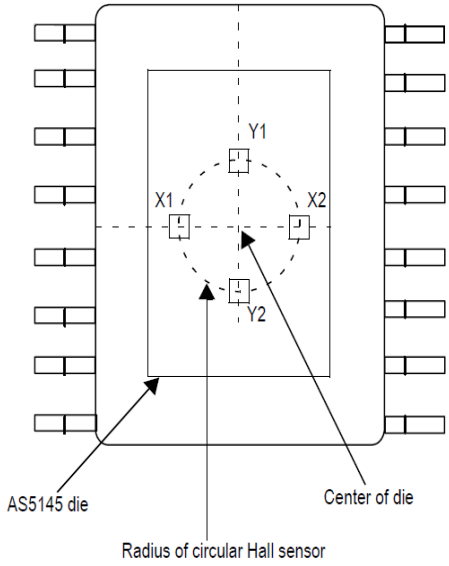

Figure 3.9: Arrangement of Hall-effect sensors on chip [2, p. 26].

Sensor summary

Table 3.2 summarizes the needs and scoring of the different position sensors. The scoring is done by considering the theory of the already implemented sensors and the development of the next prototype at BorgWarner.

		VR resolver		**Discrete Hall-effect sensor**		**Magnetic Hall-based encoder**	
Specification	Weight	Score	Weighted score	Score	Weighted score	Score	Weighted score
Cost	2	3	6	5	10	4	8
EMC performance	4	5	20	2	8	4	9
Low complexity	3	4	12	4	12	3	9
Mounting	3	4	12	3	9	1	3
Resolution	4	4	16	1	4	4	16
Robust	5	4	20	4	20	3	15
Well-known	2	5	10	5	10	3	6
		Total	**96**	**Total**	**73**	**Total**	**65**

Table 3.2: Sensor scoring table.

3.2.3 Test setup

A complete rig setup with a PMSM unit, power electronics and control and logging systems has been built. This section describes its implementation and configuration.

Power electronics

The inverters used in the test setup are based on the Infineon® HybridPACK™ 1 kit which is shown in figure 3.10. This is a complete evaluation kit for designing hybrid vehicle applications and is suitable for light-weight applications up to 20 kW and 450 V. It consist of three parts; a power module, a logic board and an adapter in between. The power module consist of six Insulated-Gate Bipolar Transistors (IGBTs) developed by Infineon®. The logic board provides a variety of control and measurement possibilities such as; phase current and temperature measurements as well as CAN, RS232 and JTAG interfaces.

Figure 3.10: Infineon HK1 [9, p. 9].

Considering the topic of this thesis, the most important interfaces are the position sensor interfaces. The logic board includes a 12-bit RDC to handle resolver outputs and resolver excitation signal [9, p. 47]. The ADC is the AD2S1200YST from Analog Devices®(see figure 3.11).

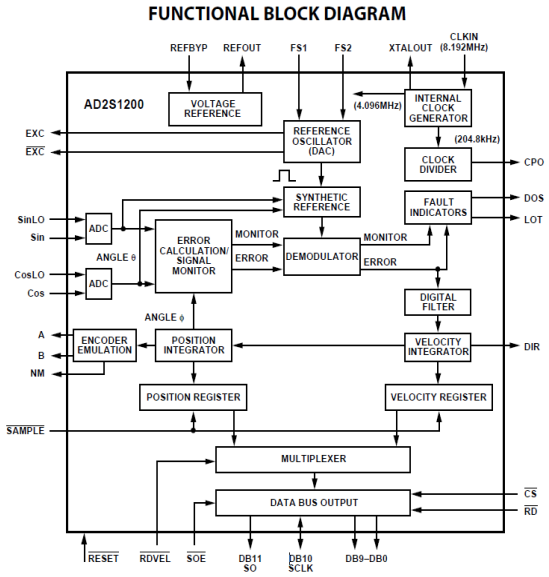

Figure 3.11: AD2S1200 functional block diagram [3, p. 1].

The Hall-effect interface is three input pins that assumes open-collector output from the sensor and consist of pull-up resistors and optional first order low-pass filters.

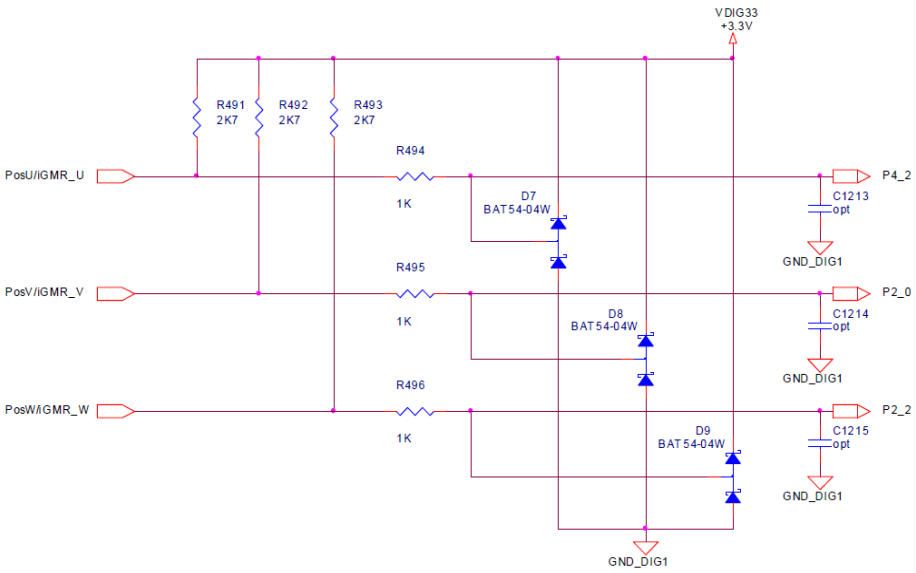

Figure 3.12: Hall-effect sensor interface [9, p. 65].

Configuration

The complete setup consist of following:

- A PMSM unit mounted in the rig.
- Power electronics based on the Infineon HK1.
- A NiMh battery of 280 V nominal and 1.3 kWh. Maximum discharging current is 140 A.
- dSPACE MicroAutoBox.
- Computer to program and monitoring the power electronics via JTAG interface.
- Computer to control and monitoring the PMSM.
- Computer to control the rig and log the measured data.

All signals are logged via the CAN bus which is running at 100 Hz. The low sampling rate means that the position signals are useless already at low speeds and the main interests will be the measured shaft torque. The hardware and software that is used to monitor and log all signals are CANCase with Vector CANAlyzer and National Instrument DIAdem. The Hall-effect interface filter coefficients are chosen to get a cutoff frequency of 2 kHz. All cables and connectors are shielded and grounded. The motor, power electronics and rig chassis are well grounded to the same grounding point.

3.3 Simulation and test cases

This section describes the test cases that are going to be performed by simulations and testings, and why this cases have been chosen. The cases are mostly considering the testing possibilities at BorgWarner.

1. Increasing torque step references with a constant rig controlled speed.
2. Square wave torque references (± 4 Nm @ 1 Hz) with minimal load (friction load) and minimal inertia.

   These cases will be done with the resolver, the Hall-effect sensor and the Hall-effect sensor with the observer enabled.

   There are some other cases that could be interesting to investigate. Due to limitations in testing possibilities and time, these following cases are only simulated.

3. Use different parameters for the Hall-effect sensor filter and evaluate torque ripple and output signal delay.
4. Evaluate the SKF bearing sensor based on real measurement data provided by SKF.

Chapter 4

Results

This chapter presents the simulation and test results. The case numbers refers to the test cases described in section 3.3. The results presents the torque response, torque ripple and torque frequency content as defined in chapter 3.

4.1 Simulation

Case 1

Figure 4.1 shows that in the case of the Hall-effect sensor, the PMSM gives lowest mean torque. The results is better with the observer and best when simulating with the resolver.

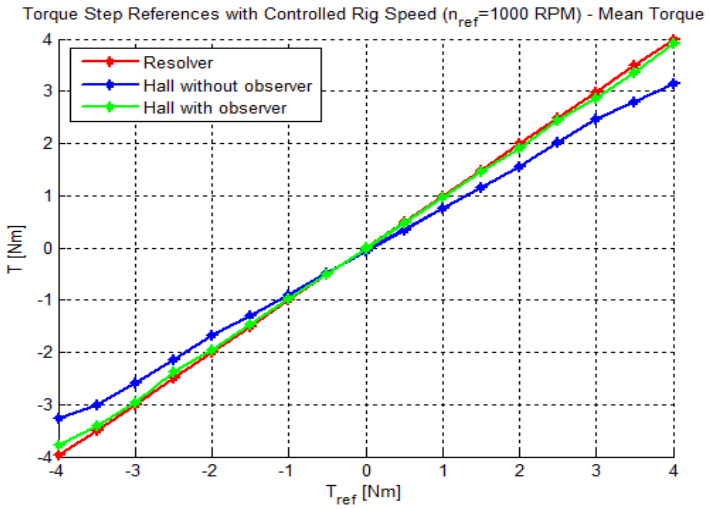

Figure 4.1: Mean torque step response using resolver and Hall-effect sensor with and without observer.

The PMSM to produce more torque ripple when running with the Hall-effect sensors, compared to the case when having the observer enabled or simulating with the resolver, as shown in figure 4.2.

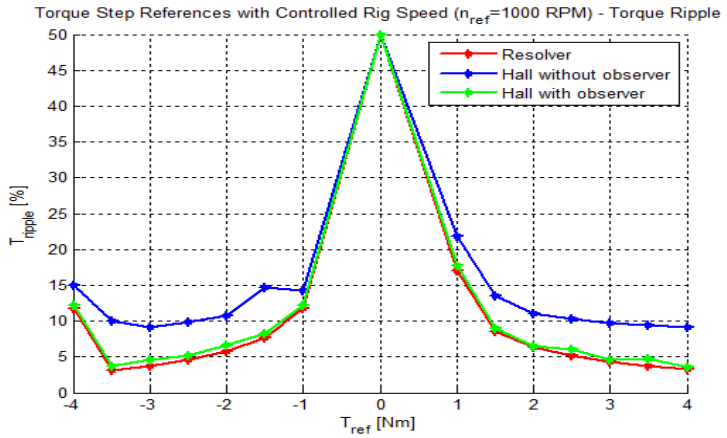

Figure 4.2: Torque ripple response using resolver and Hall-effect sensor with and without observer.

The torque ripple consist of some harmonics which is shown in figure 4.3. All sensors causes harmonics at multiples of the switching frequency, but the Hall-effect sensor has also a lot low frequency harmonics.

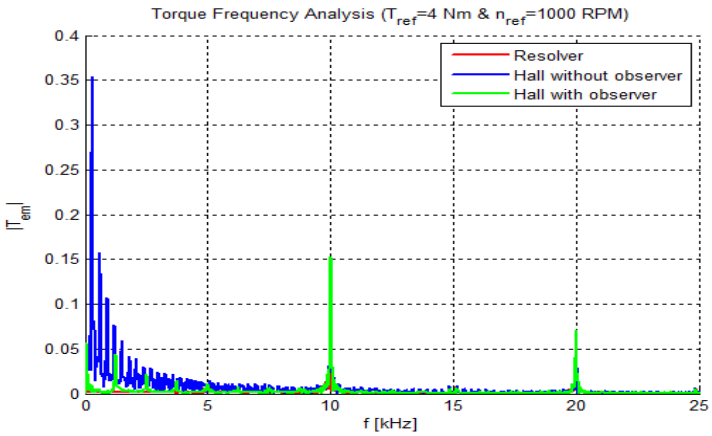

Figure 4.3: Torque ripple frequency analyse using resolver and Hall-effect sensor with and without observer.

Case 2

The simulation results from the square wave torque reference case are shown in figure 4.4, 4.5 and 4.6.

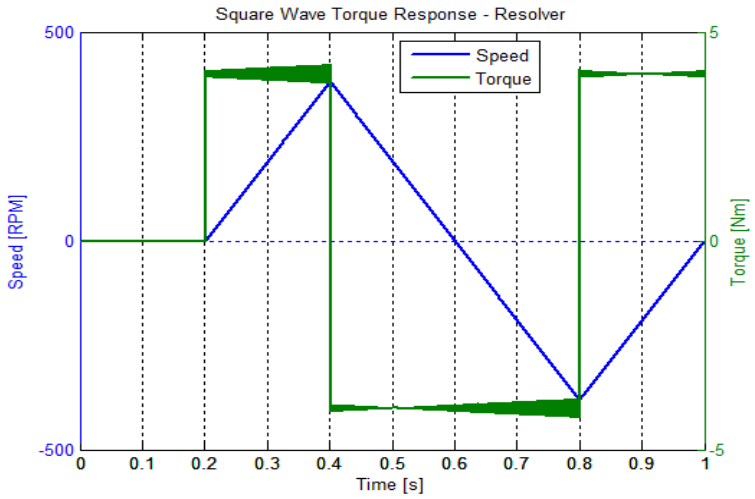

Figure 4.4: Square wave torque response and speed using resolver.

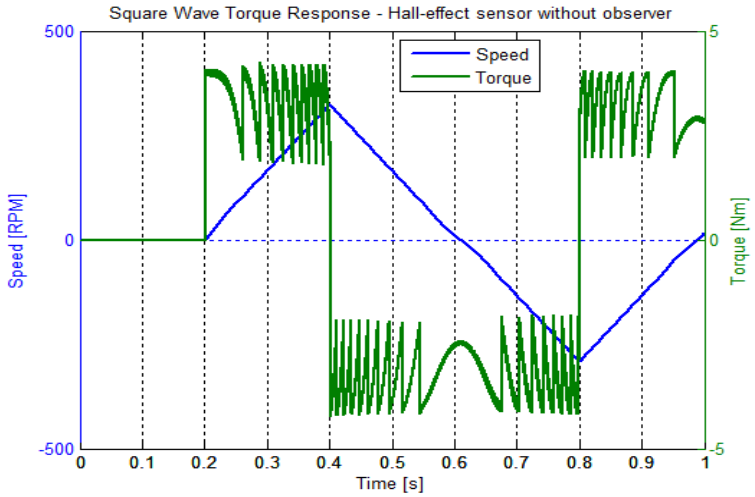

Figure 4.5: Square wave torque response and speed using Hall-effect sensor without observer.

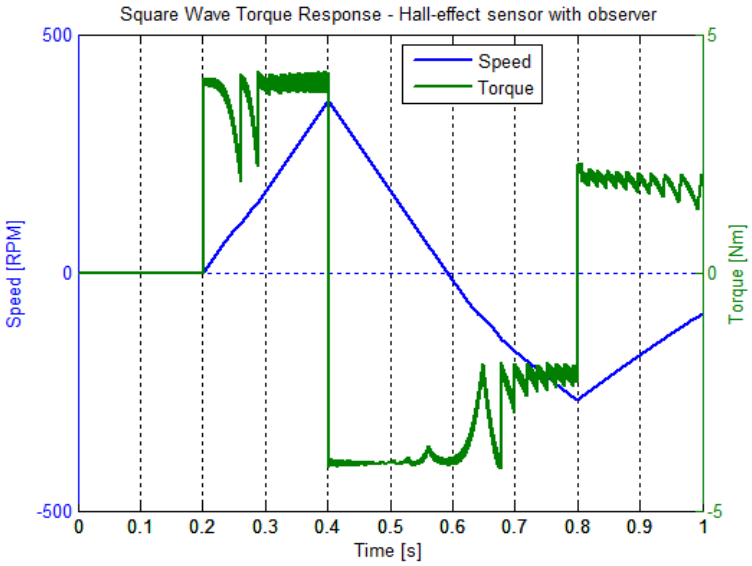

Figure 4.6: Square wave torque response and speed using Hall-effect sensor with observer.

The resolver case shows low torque ripple and good behaviour. When simulating with the Hall-effect sensor without observer enabled, there are a lot of torque ripple which frequency increases with speed. When enabling the observer the performance become a little bit better, but the prediction is bad when the PMSM passing zero speed and changing direction of rotation.

Case 3

As mentioned in the theory part, the Hall-effect sensor signals needs to be filtered and filtering introduces phase delays. How much different phase delays affects the performance of the PMSM is shown in figure 4.7.

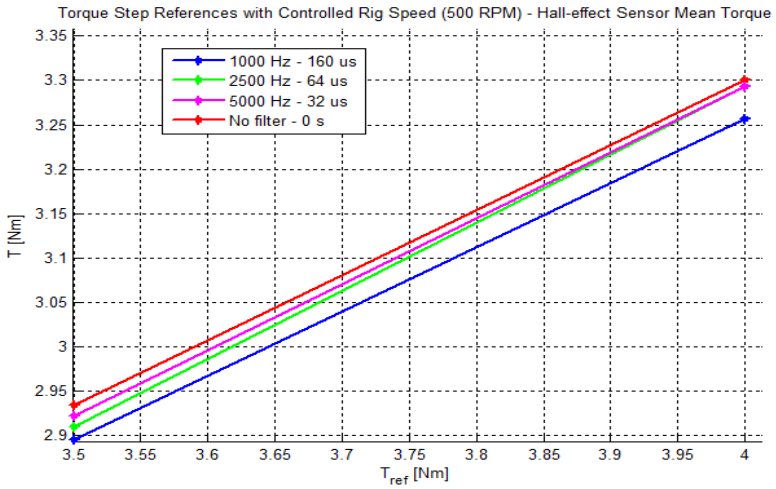

Figure 4.7: Torque response using Hall-effect sensor low-pass filtering with different cut-off frequency.

This result shows only on small differences, but is anyway affecting the system.

Case 4

The simulation results based on real measured data for the SKF bearing sensor are shown in figure 4.8, 4.9 and 4.10.

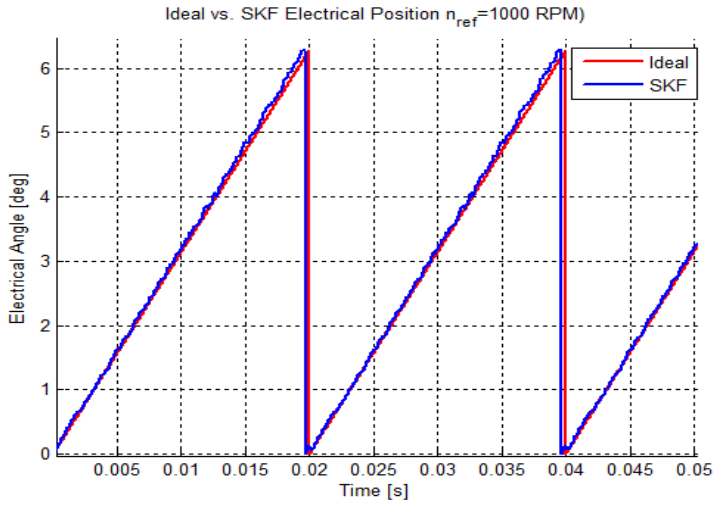

Figure 4.8: Ideal and SKF bearing sensor position comparison.

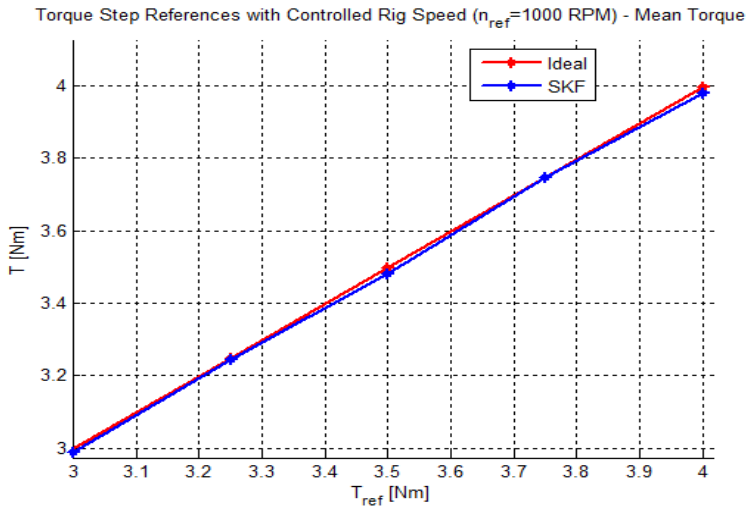

Figure 4.9: Ideal and SKF bearing sensor position mean torque response.

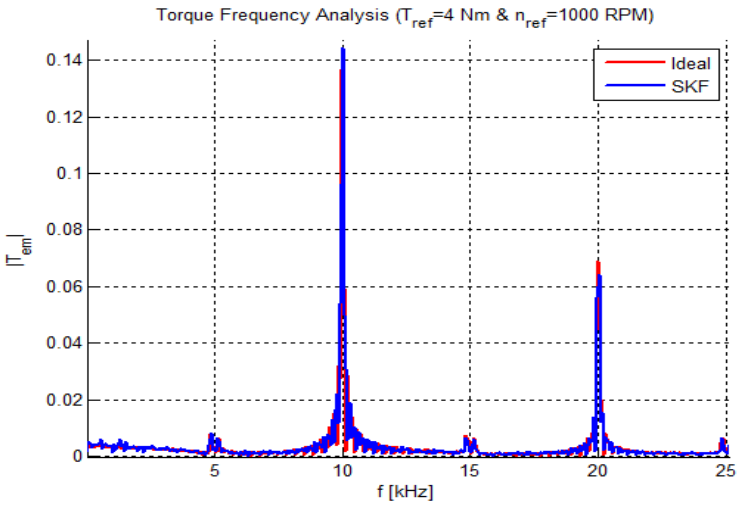

Figure 4.10: Ideal and SKF bearing sensor position frequency analyse.

The results shows only small differences between the ideal position and the SKF sensor bearing position.

4.2 Testing

The testing results shows on same behaviour as in the simulations.

Case 1

When the PMSM is running with the Hall-effect sensors, the mean torque response are lower than with observer enabled and for the resolver (see figure 4.11). Figure 4.12 shows the torque ripple for the same test case. Here are the ripple highest for the Hall-effect sensor, lower with the observer enabled and lowest when running with the resolver.

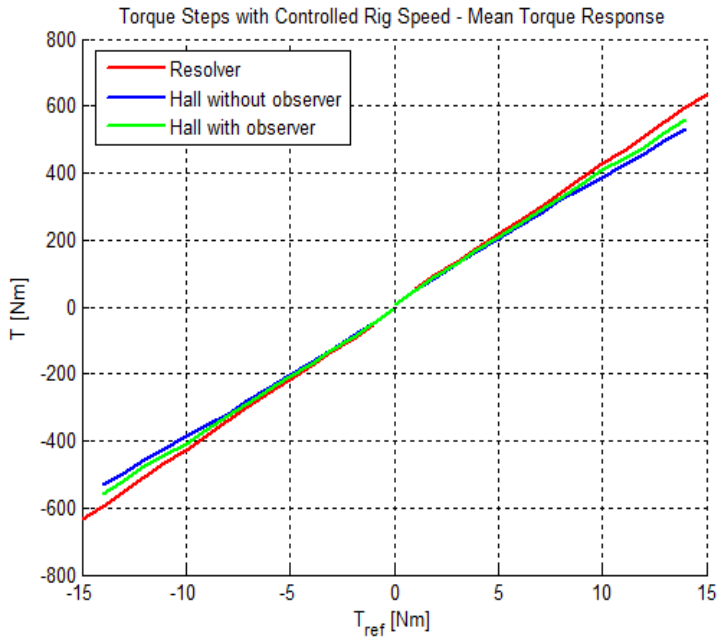

Figure 4.11: Mean torque step response using resolver and Hall-effect sensor with and without observer.

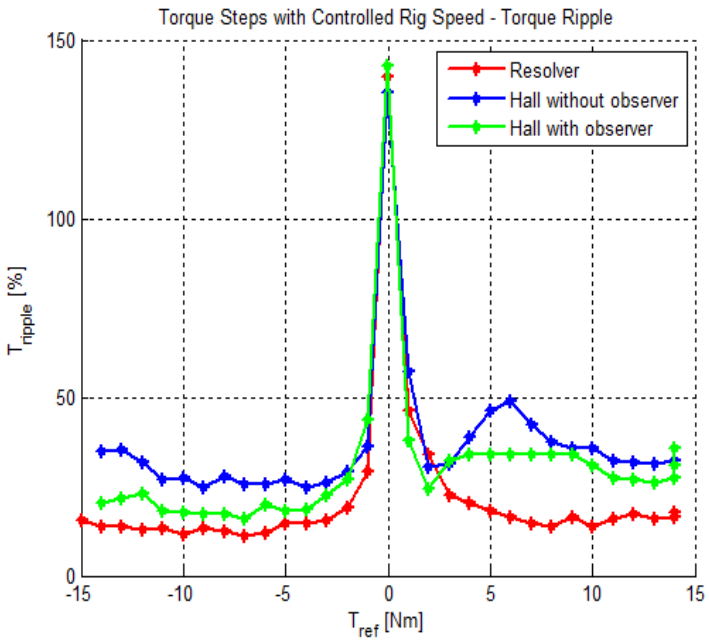

Figure 4.12: Torque ripple response using resolver and Hall-effect sensor with and without observer.

Case 2

Figure 4.13, 4.14 and 4.15 shows the test results for the square wave torque case. The overshoots when changing torque reference are due to mechanical resonances in the machine. When the machine is changing direction of rotation when running Hall-effect sensors with observer, the performance is really bad and the position prediction is not working well.

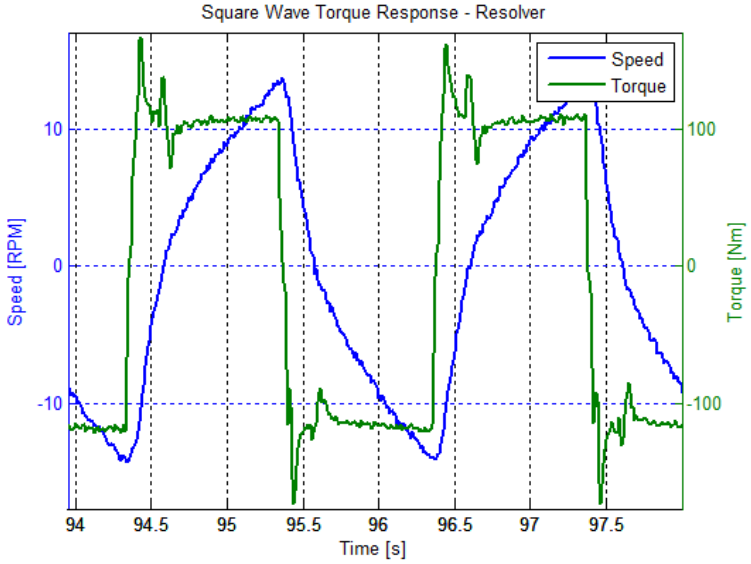

Figure 4.13: Square wave torque response and speed using resolver.

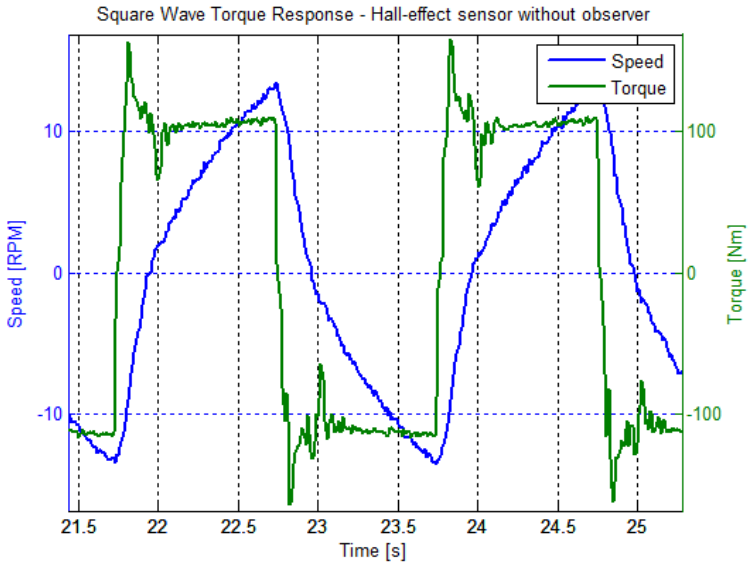

Figure 4.14: Square wave torque response and speed using Hall-effect sensor without observer.

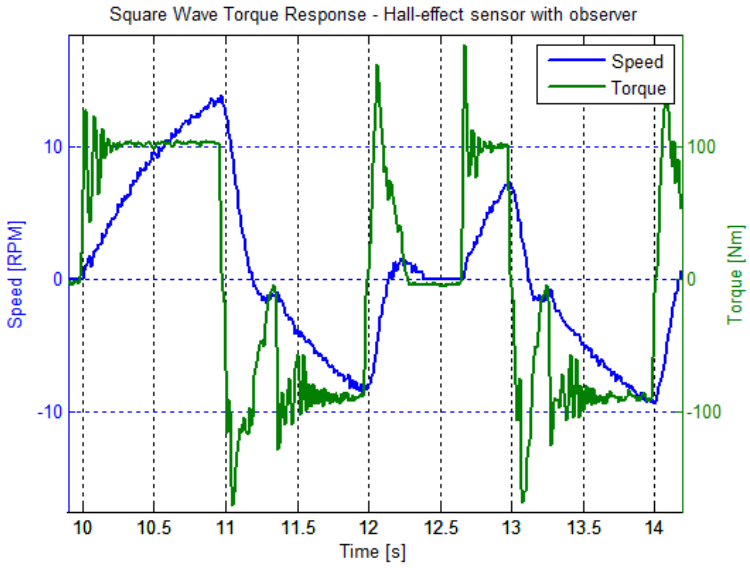

Figure 4.15: Square wave torque response and speed using Hall-effect sensor with observer.

Chapter 5

Discussion

The position sensor is a key parameter for efficient control of a PMSM and it is very important to know the right position of the rotor shaft at all time. In this type of application is it hard to compromise between performance and price since the price of the position sensor only is a fraction of the complete unit.

Both the simulation and testing results shows similar behaviour for each sensor type and the models can be said to match well together. Even if the system model are very ideal and that a real complete test system would be very difficult to model and simulate, this model can give some hints of how the choice of position sensor affects the over-all system performance. The weighted score table of the sensors that was made in section 3.2.2 resulted in highest score for the resolver.

Due to the measurements low sampling rate of 100 Hz is it not possible to see the same system behaviour that can be seen in the simulations. One example is the frequency analysis of the torque ripple where the simulation results of all sensors shows harmonics at multiples of the switching frequency (10 kHz). The Hall-effect sensor simulation shows also a lot of harmonics at multiples of 600 Hz which are induced from the sensor and that varies with the speed. The simulation model has also the advantages to run cases that are impossible to test in the rig setup, e.g. high speeds, fast accelerations and high torque load with good resolution. A drawback is that the simulation model is not affected by real world parameters as EMI and interference with other systems.

5.1 Conclusions

The results shows consistently that the PMSM gives less mean torque and more torque ripple when running with the Hall-effect sensor. With the same torque reference and with the observer activated the results are a bit better in some cases but around zero speed when changing sign of the direction fast, the performance is really bad due to poor position prediction in that case. The reason for this is be the actual implementation of the observer and that it needs a more

advanced or improved implementation. The TV application function is based on the fast changing sign of rotation direction and thus the observer may not be a good choice. The resolver showed the best results with lowest torque ripple, even if a lot of noise was measured on both excitation and position signals.

When the machine is running with the Hall-effects sensor at low speed, the machine is in between two Hall-states during a long time and thus the error in position is large during this time. This leads to larger drops in torque than when it is running faster. In other words, this results in a speed dependent torque ripple which frequency varies along with the speed. This behaviour can trigger resonances in the mechanical constructions that may cause vibrations and noise in the application.

In EV and HEV applications, EMI is a huge problem that needs to be taken into consideration in every design and construction step and when choosing components such as position sensors. Different parts of the system and construction, signals cables and all other equipment needs to be well connected and tightened to ground, but in car implementations are only a $\pm$12V reference available. The absence of a stable ground that differs a lot in potential across the chassis of the car are not good. This will influence on the operation of the position sensor due to the relatively long distance between the sensor placement in the PMSM and the power electronic. A recommendation, to avoid or decrease the influence of this problem, is to have a good physical connection between the PMSM and the power electronics box, shielded cables and connectors and as short cables as possible. Good filtering and decoupling on both supply and signal lines are also preferred.

The Hall-effect sensors low-pass filters contributes to phase delays in the position signals that increases the torque ripple and since the electrical interface consist of three signals, each with a low-pass filter, the filter parameters may not be identical in all three filters. This may give a bad non-linear behaviour in the final position value and in turn, complicates the observer functionality since the prediction is done by the average speed between the previous two states.

I had high expectations of the encoder but due to lack of time and bad designed mountings, it could not be tested. Anyway, this type of encoder could not suit the next prototype of the eAWD project since the new design makes it impossible to access and mount the encoder in line with the rotor axle.

5.1.1 Choice of sensor

The best and most well-known position sensor today is the resolver, and especially the Variable Reluctance (VR) resolver is to recommend in this type of applications. The pure discrete analog and digital Hall-effect sensor is not to recommend at all, but this technique can be used and combined in other ways than using discrete Hall-effect sensors, e.g. the Hall-effect based encoder and the SKF bearing sensor. Both the resolver and the pure Hall-effect or Hall-effect based sensors are using magnet fields to measure position. This makes it important to place the sensor in a good way so other magnet fields do not interfere. Furthermore, a sensor with a differential electrical interface is also to

recommend and a shaft-through or partial shaft-through design is needed due to the design of the next eAWD prototypes.

The resolver has been used for a long time in electrical machines. Today, the development of EV and HEV motors has accelerated and the resolver may not be the best and optimum choice when it comes to robustness, manufacturing cost, integration and reliability. The eddy-current based sensors are still new and unexplored, but these may be one of the prime choice for this type of applications in the future.

5.2 Future development

Alternative position sensors that could contribute to a lot of advantages are the SKF bearing sensor or the eddy-current based sensors. The SKF bearing sensor has the advantages to replace existing bearings and that it is not needing any excitation and modulation/demodulation (as in the case of the resolver). The results shows also on good performance but it is difficult to evaluate since the model is based on real measured data.

The Hall-effect sensor observer may be optimized or another technique as a Kalman filter can be used. The low-pass filtering of the Hall-effect signals are also very crucial, but it introduces phase delay that affects the performance. This can also be improved with a more advanced filtering, but this increases of course complexity and cost.

Bibliography

[1] Mats Alaküla and Per Karlsson. *Power Electronics - Devices, Converters, Control and Applications*. Department of Industrial Electrical Engineering and Automation, 2010.

[2] AMS. *Data Sheet - AS5145/AS5145A/AS5145B 12-Bit Programmable Magnetic Rotary Encoder*. austriamicrosystems, rev. 1.10 edition, 2009.

[3] Analog Devices. *AD2S1200 12-Bit R/D Converter with Reference Oscillator*, rev. 0 edition, 2003.

[4] Christian Ascher. Inductive rotor-position sensor for synchronous motors. *Electric and hybrid vehicle technology international*, page 189, July 2011.

[5] Oliver Brunel and Rainer Möller. Rotor position mission. *Electric and hybrid vehicle technology international*, page 147, July 2011.

[6] Machine Designers. Machine design - servomotors, stepper motors, and actuators for motion. `http://uniquemachines.blogspot.com/2010/10/servomotors-stepper-motorsand-actuators.html`, October 2010. Date of visit: 2011-07-15.

[7] Lennart Harnefors. *On analysis, control and estimation of variable-speed drives*. PhD thesis, KTH, 1997.

[8] Seon-Hwan Hwang, Hyun-Jin Kim, Jang-Mok Kim, Liming Liu, and Hui Li. Compensation of amplitude imbalance and imperfect quadrature in resolver signals for pmsm drives. *IEEE*, 2011.

[9] Infineon. *Hybrid Kit for HybridPACK 1 - Evaluation Kit for Applications with HybridPACK 1 Module*, 2.1 edition, 2010.

[10] Pierrick Mazé. Skf sensor-bearing solutions for automotive electric motors. Presented at BorgWarner TTS AB by SKF, May 2011.

[11] Taiichi Miya. Double variable reluctance resolver for multiple speed resolver system. U.S Patent No. 7,157906 B2, January 2007.

[12] Edward Ramsden. *Hall-Effect Sensors: Theory and Application*. Newnes, second edition, 2006.

[13] Funda Sahin, H. Bülent Ertan, and Kemal Leblebicioglu. Optimum geometry for torque ripple minimization of switched reluctance motors. *IEEE*, 2000.

[14] Sensing and Control. *Solid State Sensors SS400 Series*. Honeywell Inc.

[15] Martin Staebler. *TMS320F240 DSP Solution for Obtaining Resolver Angular Position and Speed*. Texas Instruments, 2000.

[16] Jason Starck. Ac instrumentation transducers. `http://www.allaboutcircuits.com/vol_2/chpt_12/6.html`, June 2000. Date of visit: 2011-04-05.

[17] SUMIDA. *Technical Information: Rotor Position Sensor*. SUMIDA Components and Modules GmbH, rev. 04 edition, 2010.

Appendix A

Technical Data Sheets

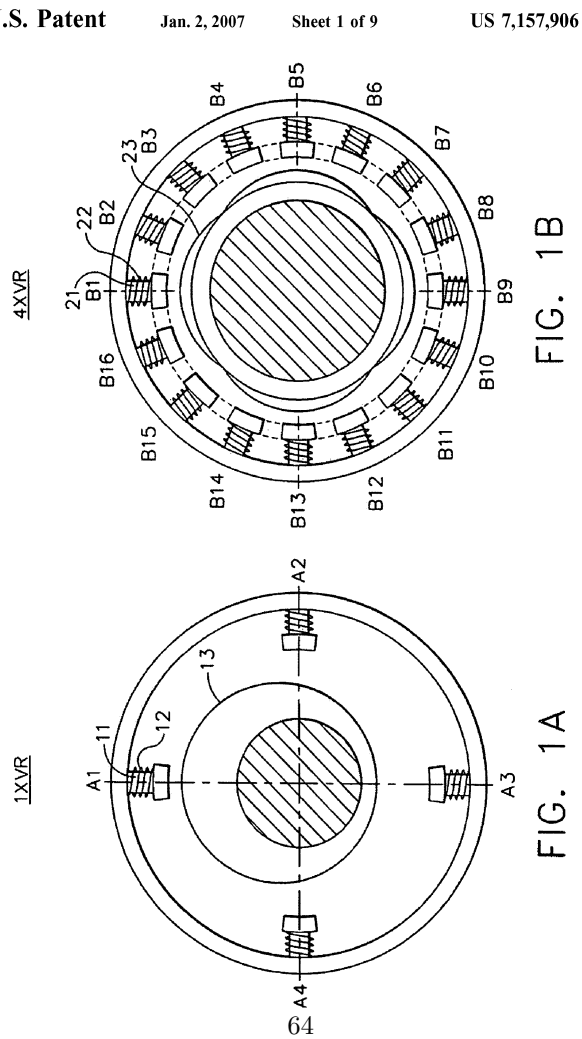

Figure A.1: Construction of two VR resolvers with different number of pole pairs. Figure 1A: 1 pole pair. Figure 1B: 4 pole pairs. [11, p. 2].